Calculation of the melting point of NaCl by molecular simulation

Jamshed Anwar[a)]
Computational Pharmaceutical Sciences, Department of Pharmacy, King's College London, Franklin-Wilkins Building, London SE1 9NN, United Kingdom

Daan Frenkel[b)]
Computational Physics, FOM Institute for Atomic and Molecular Physics, Kruislaan 407, 1098 SJ Amsterdam, The Netherlands

Massimo G. Noro[c)]
Unilever Research Port Sunlight, Quarry Road East, Bebbington, Wirral CH6 33JW, United Kingdom

(Received 5 June 2002; accepted 25 September 2002)

We report a numerical calculation of the melting point of NaCl. The solid–liquid transition was located by determining the point where the chemical potentials of the solid and liquid phases intersect. To compute these chemical potentials, we made use of free energy calculations. For the solid phase the free energy was determined by thermodynamic integration from the Einstein crystal. For the liquid phase two distinct approaches were employed: one based on particle insertion and growth using the Kirkwood coupling parameter, and the other involving thermodynamic integration of the NaCl liquid to a Lennard-Jones fluid. The latter approach was found to be significantly more accurate. The coexistence point at 1074 K was characterized by a pressure of -30 ± 40 MPa and a chemical potential of $-97.9\pm0.2k_\beta T$. This result is remarkably good as the error bounds on the pressure enclose the expected coexistence pressure of about 0.1 MPa (ambient). Using the Clausius–Clapyron relation, we estimate that $dP/dT\approx3$ MPa/K. This yields a melting point of 1064 ± 14 K at *ambient pressure*, which encompasses the quoted range for the experimental melting point (1072.45–1074.4 K). The good agreement with the experimental melting-point data provides additional evidence that the Tosi–Fumi model for NaCl is quite accurate. Our study illustrates that the melting point of an ionic system can be calculated accurately by employing a judicious combination of free energy techniques. The techniques used in this work can be directly extended to more complex, charged systems. © *2003 American Institute of Physics.*
[DOI: 10.1063/1.1522375]

I. INTRODUCTION

Solid–fluid transitions tend to be strongly first order, being characterized by an appreciable hysteresis. This can present a serious technical challenge to computer simulation of such phenomena. In principle, it is possible to search for coexistence in a simulation of a large, two-phase system. However, in such a simulation, finite-size effects, associated with the presence of an interface, are expected to be appreciable. Hence the method is limited to large systems. This, in turn, implies that such an approach is likely to be prohibitively expensive for systems consisting of complex molecules. For this reason, it is important to make use of computational techniques that locate the coexistence point through ''bulk'' simulations of the two coexisting phases. An example of such a technique is the Gibbs ensemble method[1] in which the two coexisting phases are simulated in separate but coupled simulation cells. While the Gibbs ensemble method can be applied to solids (D. T. Wu, private communication), this application of the method is still largely unexplored. An approach that has gained considerable popularity in the study of solid–fluid equilibria, is the Gibbs–Duhem integration method[2,3] that traces out the coexistence line. A drawback with this method is that to initiate the procedure, one requires knowledge of at least one point on the coexistence curve, which must be determined by some alternative means. The Gibbs–Duhem method can therefore be used only in combination with another technique to locate coexistence points.

At the solid–liquid coexistence point, the pressure and the chemical potential of the coexisting solid and liquid phases are equal. Hence, one possible route to determining the coexistence point is to calculate the chemical potential or the free energy of each phase separately as a function of pressure and thereby ascertain the intersection point at which the pressures and chemical potentials are equal. Once one such coexistence point has been determined, then, in principle, the entire coexistence line may be determined using the Gibbs–Duhem integration procedure. This approach involving the explicit calculation of the chemical potentials of the individual phases (coupled in some instances with subsequent Gibbs–Duhem integration) has been employed to investigate the phase behavior of many systems including simple models such as ellipsoids,[4] Lennard-Jones particles,[5]

a)Author to whom correspondence should be addressed. Electronic mail: jamshed.anwar@kcl.ac.uk
b)Electronic mail: frenkel@amolf.nl
c)Electronic mail: massimo.noro@unilever.com

spherocylinders,[6] two-dimensional (2D) discs as models for membrane proteins,[7] and more realistic model systems such as N_2,[8,9] CO_2,[10] N_2O,[11] and H_2O.[12,13] Recent applications of increased complexity include a realistic model of *n*-octane[14] and iron.[15]

The present study attempts to calculate the melting point of NaCl. While the melting of NaCl is interesting in its own right, our main reason for studying this substance is that it is the simplest representative of a large class of ionic materials. The same techniques that allow us to compute the melting curve of NaCl should allow us to study melting of complex organic salts and, eventually, of protein crystals. Apart from this methodological incentive, the alkali halides, of which NaCl is the archetypical member, have been extensively studied both experimentally and theoretically, and consequently have played an important role in the development of solid-state theory. The thermodynamic and structural properties of NaCl are of particular interest since it is employed extensively to assure internally consistent thermodynamic values of many other substances. For instance, the lattice parameter of NaCl serves as a secondary standard for the high-pressure scale. To our knowledge, the present calculation of the melting point of NaCl represents the first such calculation for a pure ionic system.

The main reason why the calculation of the melting point of NaCl (and ionic systems in general) is technically challenging is the presence of long-range Coulomb forces in such systems. The presence of Coulomb interactions poses technical difficulties for almost every aspect of the calculation of the free energy of the solid and the liquid. In the current study the chemical potential of the NaCl solid was determined by thermodynamic integration from the Einstein crystal. For the NaCl liquid two distinct approaches have been employed and compared. A scheme involving thermodynamic integration of a LJ fluid to NaCl fluid was found to be the most accurate.

II. THEORY

At the melting point $T_m(P)$ of a substance, the pressure and the chemical potential of the coexisting solid and liquid phases are equal. To calculate the melting point, it is therefore necessary to determine the intersection point of the chemical potentials of the solid and the liquid phase. A convenient approach is to determine the chemical potentials for the two phases as a function of density (or pressure) at a defined temperature, and to express the data in the form of empirical equations of state from which the intersection point may be calculated.

A. Chemical potential of the solid phase

The chemical potential of the NaCl solid phase was determined by thermodynamic integration using the Einstein crystal approach.[16] The Einstein crystal comprises noninteracting particles that are coupled harmonically to their equilibrium lattice sites. In the present study the Na and Cl ions were assigned separate coupling constants. The revised potential for the Einstein crystal was

$$U_E=\frac{\gamma_{\mathrm{Na}}}{2}\sum_{i=1}^{N_{\mathrm{Na}}}(\mathbf{r}_i-\mathbf{r}_{0,i})^2+\frac{\gamma_{\mathrm{Cl}}}{2}\sum_{i=1}^{N_{\mathrm{Cl}}}(\mathbf{r}_i-\mathbf{r}_{0,i})^2, \tag{1}$$

where N_{Na} and N_{Cl} are the number of ions of each type, γ_{Na} and γ_{Cl} are the associated force constants characterizing the strength of the coupling, and $\mathbf{r}_{0,i}$ is the equilibrium lattice position of particle i.

For technical reasons (detailed in Refs. 17 and 18), it is important to fix the center-of-mass position of the system in the thermodynamic integration from the Einstein crystal. This necessitates a finite system-size correction associated with the center-of-mass constraint. There are thus three components to the free energy of the solid phase: the absolute free energy of an Einstein crystal with a center-of-mass constraint $F_{\mathrm{E(CM)}}$, the free energy change for the thermodynamic integration from the Einstein crystal to NaCl (with the center-of-mass constraint) $\Delta F_{\mathrm{E(CM)}\rightarrow\mathrm{NaCl(CM)}}$, and the finite system-size correction associated with the applied center-of-mass constraint $\Delta F_{\mathrm{NaCl(CM)}\rightarrow\mathrm{NaCl}}$. Hence

$$F_{\mathrm{solid}}=F_{\mathrm{E(CM)}}+\Delta F_{\mathrm{E(CM)}\rightarrow\mathrm{NaCl(CM)}}+\Delta F_{\mathrm{NaCl(CM)}\rightarrow\mathrm{NaCl}}, \tag{2}$$

where CM specifies that the center of mass is constrained.

For NaCl with the two ions having a distinct lattice-coupling force constant, the various free-energy components per NaCl ion pair take the following explicit forms:

$$\begin{aligned}\frac{\beta F_{\mathrm{E(CM)}}}{N_{\mathrm{NaCl}}}=&3\ln\Lambda_{\mathrm{Na}}+3\ln\Lambda_{\mathrm{Cl}}-\frac{3N_{\mathrm{Na}}}{2N_{\mathrm{NaCl}}}\ln\left(\frac{2\pi}{\beta\gamma_{\mathrm{Na}}}\right)\\&-\frac{3N_{\mathrm{Cl}}}{2N_{\mathrm{NaCl}}}\ln\left(\frac{2\pi}{\beta\gamma_{\mathrm{Cl}}}\right)-\frac{3}{2N_{\mathrm{NaCl}}}\ln\left(\frac{\beta\gamma_{\mathrm{Na}}}{2\pi N_{\mathrm{Na}}\mu_{\mathrm{Na}}^2}\right)\\&-\frac{3}{2N_{\mathrm{NaCl}}}\ln\left(\frac{\beta\gamma_{\mathrm{Cl}}}{2\pi N_{\mathrm{Cl}}\mu_{\mathrm{Cl}}^2}\right)\\&-\frac{3}{2N_{\mathrm{NaCl}}}\ln\left(\frac{\beta h^2}{2\pi(N_{\mathrm{Na}}m_{\mathrm{Na}}+N_{\mathrm{Cl}}m_{\mathrm{Cl}})}\right),\end{aligned} \tag{3}$$

$$\frac{\beta\Delta F_{\mathrm{E(CM)}\rightarrow\mathrm{NaCl(CM)}}}{N_{\mathrm{NaCl}}}=\frac{\beta}{N_{\mathrm{NaCl}}}\int_0^1 d\lambda\langle U_{\mathrm{NaCl}}-U_E\rangle, \tag{4}$$

$$\begin{aligned}\frac{\beta\Delta F_{\mathrm{NaCl(CM)}\rightarrow\mathrm{NaCl}}}{N_{\mathrm{NaCl}}}=&\frac{1}{N_{\mathrm{NaCl}}}\ln\left(\frac{N_{\mathrm{NaCl}}}{V}\right)\\&+\frac{3}{2N_{\mathrm{NaCl}}}\ln\left(\frac{\beta h^2}{2\pi(N_{\mathrm{Na}}m_{\mathrm{Na}}+N_{\mathrm{Cl}}m_{\mathrm{Cl}})}\right)\end{aligned} \tag{5}$$

in which h is Planck's constant, $\beta=1/k_\beta T$, N_{Na} and m_{Na} and N_{Cl} and m_{Cl} are the numbers of particles and masses of the sodium and chloride ions, respectively, N_{NaCl} the number of NaCl ion pairs, $\mu_i=m_i/\Sigma_i m_i$ the fractional mass of each species, and Λ_i are the de Broglie wavelengths given by $\Lambda_i=h/\sqrt{2\pi m_i k_B T}$ for each ion species i.

B. Chemical potential of the liquid phase

For the liquid phase, the appropriate reference state is the ideal gas phase comprising noninteracting particles. The implication is that the chemical potential of a liquid can be calculated using a number of distinct approaches. The most

common and direct approach is to carry out thermodynamic integration above the critical temperature (to avoid any first-order transition) as a function of density by expanding the system to zero density, i.e., to an ideal gas. For NaCl, this approach is likely to be problematic. The long-range nature of the charge–charge interaction between the particles will persist even at very low densities. An alternative approach is to calculate the chemical potential directly by using the particle insertion method.[19] This method, however, is only effective at low densities. A possible combined approach could be to carry out the thermodynamic integration to low density and then employ particle insertion. A further variation is to insert an ideal gas molecule into the liquid and to grow it using the coupling parameter approach.[20]

In the present study we have explored the use of two distinct approaches for calculating the chemical potential of the NaCl liquid. In the first approach, an NaCl ion pair is grown in the liquid using the coupling parameter approach, which directly yields the chemical potential of the system. The transformation of the ideal gas ion pair into an NaCl ion pair could be carried out by gradually switching on together both the van der Waals (VDW) parameters and the charges, or in two stages by switching the van der Waals parameters first followed by the charges. Both procedures were attempted in the present study. For the single-stage process the free energy of the NaCl liquid is

$$F_{\text{liquid}} = \mu^{\text{id}} + \mu^{\text{ex}} - \frac{PV}{N_{\text{NaCl}}}, \tag{6}$$

where μ^{id} and μ^{ex} are the ideal and the excess chemical potential components. For an isothermal–isobaric ensemble the ideal part takes the form[21]

$$\beta\mu^{\text{id}}(N,P,T) = 3\ln\Lambda_{\text{Na}} + 3\ln\Lambda_{\text{Cl}} + 2\ln\left(\frac{N_{\text{NaCl}}+1}{\langle V\rangle_{N,P,T}}\right), \tag{7}$$

where $\langle V\rangle$ is the expectation value of the volume V of the (N, P, T) system. The excess chemical potential component for an isothermal–isobaric ensemble is given by the integration

$$\beta\mu^{\text{ex}}(N,P,T) = \int_{\lambda=0}^{\lambda=1} d\lambda \left\langle \frac{\partial U(\lambda)}{\partial\lambda}\right\rangle_{\lambda,NPT}. \tag{8}$$

In the two-stage procedure the above thermodynamic integration is split into two components: growth of the ideal gas particles into VDW particles, and transformation of the VDW particles into a NaCl ion pair. These simulations involving insertion and growth of a NaCl ion pair were carried out in the isothermal–isobaric ensemble to minimize N-dependence effects.

The second distinct approach involved thermodynamic integration in which a Lennard-Jones fluid is transformed into NaCl liquid at 1074 K, followed by the determination of the chemical potential of the Lennard-Jones fluid using the overlapping probability distribution method.[22] In this case the free energy of the NaCl liquid (in a NVT ensemble) is given by

$$F_{\text{liquid}} = F^{\text{id}} + F^{\text{ex}}_{\text{LJ}} + \Delta F_{\text{LJ}\rightarrow\text{NaCl}}, \tag{9}$$

where F^{id} is the ideal-gas free energy component per NaCl ion pair for the binary mixture of Na and Cl ions

$$\frac{\beta F_{\text{id}}}{N_{\text{NaCl}}} = 3\ln\Lambda_{\text{Na}} + 3\ln\Lambda_{\text{Cl}} - 2\ln\rho - 2, \tag{10}$$

where $\rho = N_{\text{NaCl}}/V$.

The excess free energy of the Lennard-Jones fluid, $\beta F^{\text{ex}}_{\text{LJ}}$, per NaCl ion pair was calculated using the overlapping probability distribution method that encompasses both particle insertions and removals using the relationship

$$\frac{\beta F^{\text{ex}}_{\text{LJ}}}{N_{\text{NaCl}}} = \frac{N}{N_{\text{NaCl}}}(\ln g(\Delta U) - \ln f(\Delta U) + \beta\Delta U) - \frac{\beta PV}{N_{\text{NaCl}}}, \tag{11}$$

where $f(\Delta U)$ and $g(\Delta U)$ are the probability distributions of the interaction energy ΔU of the inserted test particle and the removed particles, respectively.

The free energy for the thermodynamic integration of a Lennard-Jones fluid to the NaCl liquid in its explicit form is

$$\frac{\beta\Delta F_{\text{LJ}\rightarrow\text{NaCl}}}{N_{\text{NaCl}}} = \int_{\lambda=0}^{\lambda=1} d\lambda \langle U_{\text{NaCl}} - U_{\text{LJ}}\rangle_{\lambda}. \tag{12}$$

C. Location of the melting point

The free energies per NaCl ion pair for the solid and liquid phase were calculated at their respective equilibrium densities at the temperature 1074 K, which is close to the experimental melting point for NaCl at ambient pressure. To determine the free energy at a density other than that initially selected, we need to know the density dependence of the pressure for the two phases at 1074 K. For both the solid and the liquid phase, the $P(\rho)$ isotherm was described by a quadratic polynomial $P(\rho) = a + b\rho + c\rho^2$. If ρ^* denotes the density at which the free energy of the given phase has been determined, then the chemical potential $\mu(\rho)$ at some other density along the same isotherm is given by

$$\beta\mu(\rho) = \frac{\beta F^*}{N_{\text{NaCl}}} + \beta\left(2c\rho + b(\ln\rho + 1) - c\rho^* - b\ln\rho^* + \frac{a}{\rho^*}\right), \tag{13}$$

where F^* is the free energy of either the liquid or the solid phase of NaCl at 1074 K at ambient pressure.

The melting point of NaCl was located graphically, being the intersection point of plots of the chemical potentials of the liquid and the solid phase as a function of pressure at the fixed temperature of 1074 K.

III. SIMULATION DETAILS

The system contained 512 particles (256 Na and 256 Cl). For the solid phase, this is equivalent to $4\times4\times4$ unit cells. The ion–ion interaction potential was of the Born–Mayer–Huggins–Fumi–Tosi (BMHFT) form

TABLE I. Potential parameters for NaCl.

	A_{ij}/ kJ mol^{-1}	B/ Å^{-1}	C_{ij}/ Å^6 kJ mol^{-1}	D_{ij}/ Å^8 kJ mol^{-1}	σ_{ij}/ Å
Na–Na	25.4435	3.1546	101.1719	48.1771	2.340
Na–Cl	20.3548	3.1546	674.4793	837.0770	2.755
Cl–Cl	15.2661	3.1546	6985.6786	14 031.5785	3.170

$$U_{ij}=A_{ij}\exp[B(\sigma_{ij}-r)]-\frac{C_{ij}}{r^6}-\frac{D_{ij}}{r^8}+\frac{q_iq_j}{r}. \tag{14}$$

The parameters were from Tosi and Fumi[23,24] transformed for use in the above form of the potential and are given in Table I.

The non-Coulombic part of BHMFT potential was truncated at 9.0 Å but tail corrections were included to correct for the truncation. The Coulomb interaction term was evaluated using Ewald summation at a precision of 10^{-5} ($\gamma=3.5$, 8 k vectors). All the calculations were carried out using molecular dynamics utilizing the in-house software *ATOMH*.[25] The NaCl solid calculations were carried out in the *NVT* ensemble. The thermodynamic integration involving particle insertion and growth was carried out in the *NPT* ensemble, while the thermodynamic integration of the LJ fluid to NaCl liquid employed *NVT*. In the particle insertion and growth studies the system comprised 255 NaCl ion pairs in the liquid phase plus the one inserted ion pair. The timestep was 2 fs. Typically, simulation runs were of 200 ps, of which the first 80 ps were equilibration and the last 120 ps were used for the averages. The averages and associated uncertainties were calculated using the block averaging technique[26] to minimize correlation errors.

Suitable choices for the force constants γ for the Einstein crystal thermodynamic integration were determined from an *NPT* simulation using the Parrinello–Rahman boundary conditions[27] at 1074 K and were $\gamma_{\mathrm{Na}}=80.7890$ kJ mol^{-1} Å^{-2} and $\gamma_{\mathrm{Cl}}=85.0095$ kJ mol^{-1} Å^{-2} for the two species. They were calculated from the mean square displacements of the atoms using the relationship

$$\frac{3}{\beta\gamma}=\left\langle\frac{1}{N}\sum_{i=1}^{N}(\mathbf{r}_i-\mathbf{r}_{0,i})^2\right\rangle. \tag{15}$$

In general, the presence of tethering forces restraining the displacements of all particles, is incompatible with the conservation of the total momentum of a system in an MD simulation. However, we chose the harmonic force constants such that they were proportional to the respective masses of the ions. This choice ensures that the net force on the center of mass of system is zero, provided that it is initially zero. Hence the center of mass remains fixed.

For the thermodynamic integration from a Lennard-Jones fluid to the NaCl liquid, it is essential to choose liquid state points where the two models are structurally as similar as possible, and to select a reversible pathway along which there is no possibility of a first order phase transition. The selected LJ state point was $\rho^*=0.383$ and $T^*=2.0$ (where $\rho^*=\rho\sigma^3$ and $T^*=kT/\varepsilon$) with the parameters being $\sigma=2.32$ Å and $\varepsilon=4.465$ kJ mol^{-1}. This choice results from the desire to stay in the supercritical region of the LJ fluid, and an attempt to ensure that the first peak in the $g(r)$ of the LJ fluid occurs at the same position as the Na–Cl ion pair correlation peak in the NaCl liquid (see Fig. 1).

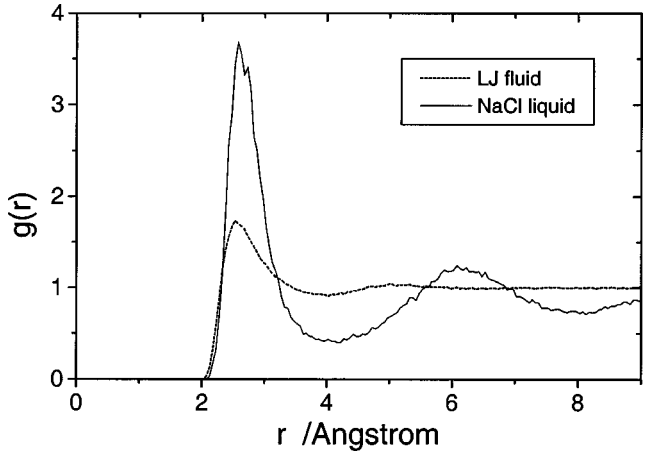

FIG. 1. Radial distribution function for a LJ fluid with parameters $\sigma=2.32$ Å and $\varepsilon=4.465$ kJ mol^{-1} (state point $\rho^*=0.383$ and $T^*=2.0$), and the Na–Cl pair interaction in NaCl liquid, both at 1074 K and 0.1 MPa pressure. The LJ fluid and the NaCl liquid represent the two states connecting the thermodynamic integration pathway employed to calculate the free energy of the NaCl liquid phase. The plot shows that the first peak for both pair interactions are almost coincident, and hence confirms the correct choice of LJ parameters that were selected to minimize the structural disparity between the two states.

IV. RESULTS AND DISCUSSION

Although proposed in the early 1960s, the Tosi–Fumi parameters[23,24] for NaCl still continue to be used in classical simulations. While the aim here is not to test the suitability of these parameters, it is important to get some idea of the parameter-related variability in thermodynamic and structural properties and its possible effect on the melting point of NaCl. The ability to reproduce basic data can also give confidence in the simulation code. On the whole the Tosi–Fumi parameters have been found to be good in reproducing the basic properties of the solid phase of NaCl. The agreement between the calculated and the experimental lattice energies at 298 K and ambient pressure is very good, the calculated energy being -770.02 kJ mol^{-1}/ion pair compared with the experimental value of -769 kJ mol^{-1}/ion pair.[28] The fusion energy too is reasonably well reproduced, the calculated value being 27.95 kJ mol^{-1}/ion pair compared with the experimental values of 28.80 kJ mol^{-1}/ion pair[29] and 28.16 kJ mol^{-1}/ion pair.[30] As for the lattice parameters, the percentage deviation is low being only 0.7%. The calculated lattice parameter is 5.682 Å while the experimental value is 5.642 Å.[31] An additional test of the potential parameters was a comparison of the calculated and experimental mean squared displacements of the ions. The mean squared displacements can be estimated from the Debye–Waller temperature factor B_j using the relationship

$$\Delta r^2=\frac{B_j}{8\pi^2}. \tag{16}$$

TABLE II. Calculated free energy components in $k_\beta T$/ion pair for the various schemes employed to determine the free energy of the crystal and the liquid phase of NaCl at 1074 K and 0.1 MPa. The terms $\beta\mu^{ex(1)}(N,P,T)$ and $\beta\mu^{ex(2)}(N,P,T)$ in column 4 are the excess free energy components for the transformation (by thermodynamic integration) of two inserted ideal-gas particles into VDW particles and the transformation of two VDW particles into an NaCl ion pair, respectively.

Einstein crystal		Liquid LJ system→NaCl		Liquid single-step ion-pair insertion and growth		Liquid two-step ion-pair insertion and growth	
$\frac{\beta F_{E(CM)}}{N_{NaCl}}=$	-13.40	$\frac{\beta F^{id}}{N_{NaCl}}=$	-24.22	$\beta\mu^{id}(N,P,T)=$	-22.22	$\beta\mu^{id}(N,P,T)=$	-22.22
$\frac{\beta\Delta F_{E(CM)\rightarrow NaCl(CM)}}{N_{NaCl}}=$	-84.72 ± 0.02	$\frac{\beta F^{ex}_{LJ}}{N_{NaCl}}=$	-0.86	$\beta\mu^{ex}(N,P,T)=$	-77.49 ± 1.00	$\beta\mu^{ex(1)}(N,P,T)=$	8.69 ± 0.21
$\frac{\beta\Delta F_{NaCl(CM)\rightarrow NaCl}}{N_{NaCl}}=$	0.37	$\frac{\beta\Delta F_{LJ\rightarrow NaCl}}{N_{NaCl}}=$	-72.65 ± 0.03			$\beta\mu^{ex(2)}(N,P,T)=$	-85.67 ± 1.00
				$-\frac{\beta P\langle V\rangle}{N_{NaCl}}=$	<0.01	$-\frac{\beta P\langle V\rangle}{N_{NaCl}}=$	<0.01
Total	-97.75 ± 0.02		-97.73 ± 0.03		-99.71 ± 1.00		-99.20 ± 1.00

The B_j values can be estimated from crystal structure refinement. For NaCl, the data at 1 bar reported by Finger and King[32] yields the experimental values $\Delta r^2_{Na}=0.020$ Å^2 and $\Delta r^2_{Na}=0.017$ Å^2. The corresponding mean squared displacements at 298 K and 1 bar from simulation are $\Delta r^2_{Na}=0.054$ Å^2 and $\Delta r^2_{Cl}=0.050$ Å^2. This is clearly a large discrepancy; the simulation values are about twofold higher than the experimental estimates. The problem here may lie with the experimental estimates. The B_j are merely adjustable parameters in the refinement of the crystal structure and are likely to include other effects such as thermal diffuse scattering.

The results for the calculations of the free-energy components for the solid and the liquid phase are tabulated in Table II. For completeness, the free energy values include the kinetic terms involving the thermal wavelengths ($3\ln\Lambda_{Na}+3\ln\Lambda_{Cl}$) even though these are identical for both the liquid and the solid phase.

The free energy of the solid phase at 1074 K and 0.1 MPa pressure determined using the Einstein crystal as the reference phase was calculated to be $-97.75\pm0.02k_\beta T$/ion pair. The thermodynamic integration of the Einstein crystal to the NaCl solid phase is displayed in Fig. 2 where $\langle U_{NaCl}-U_{Einstein}\rangle_\lambda$ is shown plotted as a function of the coupling parameter λ. The sampling points in λ were defined by a 10-point Gauss–Legendre integration scheme that was used for the integration. The high precision of the calculation is apparent from the small error bars representing the standard deviations on the ensemble average $\langle U_{NaCl}-U_{Einstein}\rangle_\lambda$.

The free energies of the liquid phase using the three different thermodynamic integration schemes (i) ion-pair insertion and growth in NaCl liquid with both VDW parameters and charges being switched on together, (ii) ion-pair insertion and growth in NaCl liquid in two stages with VDW parameters being switched on first and then followed by the charges, and (iii) thermodynamic integration of LJ fluid to NaCl liquid, were -99.7 ± 1.0, -99.2 ± 1.0, and $-97.73\pm0.03k_\beta T$/ion pair ($T=1074$ K), respectively. The particle insertion schemes, while internally consistent, are clearly both inaccurate and imprecise. The chemical potential values obtained using these schemes show a systematic error of about $-2k_\beta T$/ion pair in comparison with the values calculated for both the solid phase and the liquid phase using scheme (iii). In contrast, the value obtained using scheme (iii) is entirely consistent with that obtained for the solid phase, as are the associated (markedly lower) error estimates.

The thermodynamic integration plots for the particle insertion schemes are given in Figs. 3 and 4. Both figures reveal that the problem occurs at the initial insertion and early growth stage (low λ) of the inserted ion pair. At low λ, the inserted particles are small and get close to the other particles. This results in many close contacts between the particles that yield very large contributions to ΔU. The particle-growth simulations also showed another interesting artifact. Sometimes, the values $dU/d\lambda$ in a single simulation would exhibit a bimodal distribution. To be more precise, $dU/d\lambda$ would appear to converge, then show a discontinuity, and then convergence to a new value. The cause here is the clustering of the two inserted, small particles. This effect was

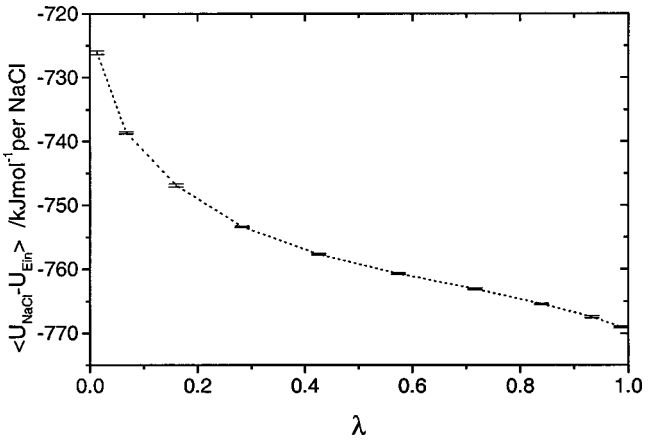

FIG. 2. Thermodynamic integration of an Einstein crystal to a NaCl crystal at 1074 K and 0.1 MPa pressure showing $\langle U_{NaCl}-U_{Einstein}\rangle_\lambda$ as a function of the coupling parameter λ. The sampling points in λ were defined by a 10-point Gauss–Legendre integration scheme that was used for the integration. The error bars represent the standard deviation in the ensemble average determined by block averaging.

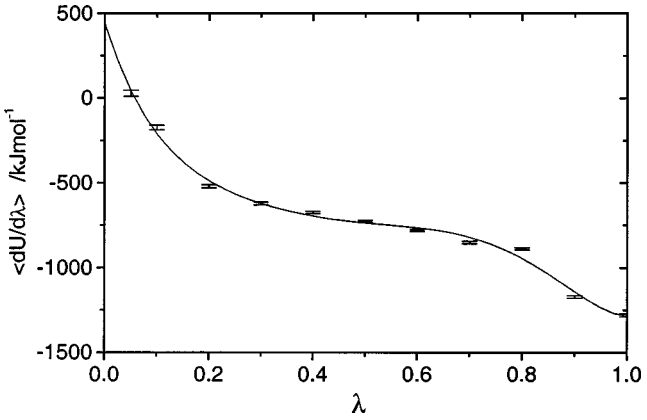

FIG. 3. Thermodynamic integration of two inserted ideal-gas particles to a NaCl ion pair (one-step procedure) in NaCl liquid at 1074 K and 0.1 MPa pressure showing $\langle U_{\mathrm{NaCl}}-U_{\mathrm{id}}\rangle_\lambda$ as a function of the coupling parameter λ. The trend line shows a sixth order polynomial fitted to the data, which was used for the integration of the plot. The error bars represent the standard deviation in the ensemble average determined by block averaging.

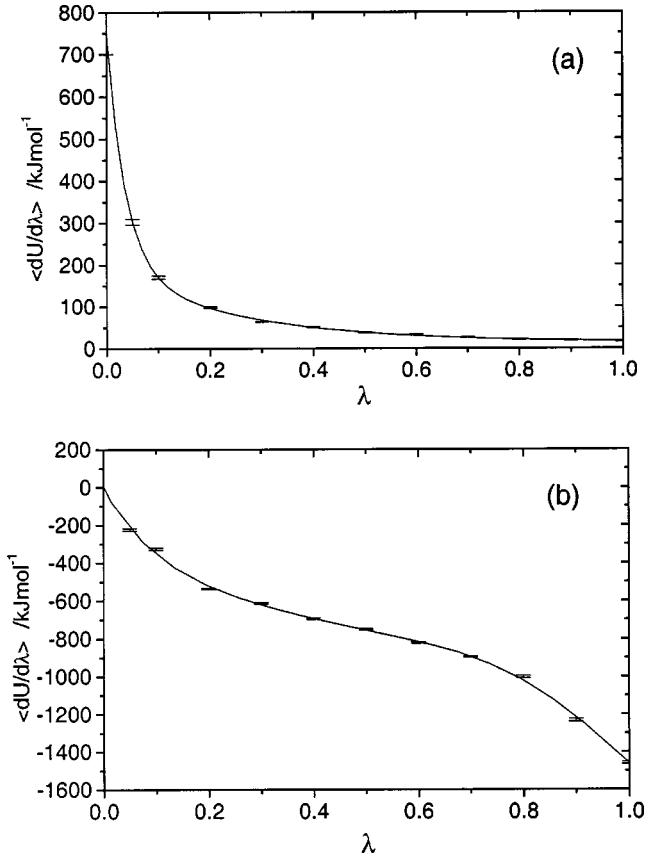

FIG. 4. Thermodynamic integration of two inserted ideal-gas particles to a NaCl ion pair in NaCl liquid at 1074 K and 0.1 MPa pressure carried out in two stages: (a) transformation of the two ideal-gas particles into two VDW particles, i.e., gradual switching on of the van der Waals parameters, and (b) transformation of the two VDW particles into a NaCl ion pair, i.e., gradual switching on of the Coulomb charges. The plots show (a) $\langle U_{\mathrm{VDW}}-U_{\mathrm{id}}\rangle_\lambda$ and (b) $\langle U_{\mathrm{NaCl}}-U_{\mathrm{VDW}}\rangle_\lambda$ as a function of the coupling parameter λ along with the fitted curves that were used for the integration of the plots. The data in (a) was fitted with a second order exponential decay equation of the form $y(x)=a0+a1\ \exp(-x/t1)+a2\ \exp(-x/t2)$ where $a0$, $a1$, $a2$, $t1$, and $t2$ are coefficients, while that in (b) was fitted with a sixth order polynomial. The error bars represent the standard deviation in the ensemble average determined by block averaging.

not investigated any further because it is simply an indication of the breakdown of this particular thermodynamic integration scheme. Fortunately, the alternative approach described below did not suffer from this problem.

The thermodynamic integration of the LJ fluid to NaCl liquid is displayed in Fig. 5 showing $\langle U_{\mathrm{NaCl}}-U_{\mathrm{LJ}}\rangle_\lambda$ as a function of the coupling parameter λ. In contrast to the particle insertion schemes, the standard deviations on the ensemble averages in this case are significantly lower. This integration is well behaved yielding accurate results, the free energy of the liquid being close to the free energy determined for the solid phase. The advantage here is that no particle creation is involved, nor are there any peculiar ion-pairing effects, as all particles in the system at any given λ have the same character.

Other than the free energies of the solid and liquid phase at 1074 K, the additional required free energy contribution is that resulting from the need to equate the pressure in the two phases at coexistence. The isotherms for both the solid and liquid phase were fitted with quadratic polynomials, i.e., $P(\rho)=a+b\rho+c\rho^2$, over the limited range of densities examined. With P in units of Pa and ρ defined as N_{NaCl}/m^3, the fitted coefficients were $a=2.601\,06\times10^{10}$ Pa, $b=-3.246\,43\times10^{-18}$ Pa m^3, $c=9.841\,11\times10^{-47}$ Pa m^6 for the solid phase, and $a=7.213\,78\times10^{9}$ Pa, $b=-1.152\,81\times10^{-18}$ Pa m^3, $c=4.460\,31\times10^{-47}$ Pa m^6 for the liquid phase.

The solid–fluid coexistence point, given by the intersection of the chemical potential of the solid and the liquid as a function of pressure, is shown in Fig. 6. The chemical potentials are displayed in terms of bounds representing an uncertainty interval of $\pm\sigma$. The intersection occurs at about -30 ± 40 MPa with μ of $-97.9\pm0.2k_\beta T$. This result is remarkably good. The selected temperature of the study is 1074 K that lies within the range of quoted experimental values for the melting point of NaCl at ambient pressure: 1073.15,[33,34] 1074.4,[35] 1072.45,[36] and 1073.2 K.[29] Consequently, at this temperature the coexistence pressure is expected to be the ambient pressure, namely about 0.1 MPa. Considering the estimated uncertainty in the calculation the $\pm\sigma$ bounds on the calculated coexistence pressure indeed enclose the expected pressure.

Given the calculated melting point, one could proceed to trace the coexistence curve using Gibbs–Duhem integration. This was not attempted due to lack of melting point data as a function of pressure. It is, however, useful to examine how the melting point varies (locally) as a function of pressure about the calculated melting point, and to estimate how the error bounds in pressure translate to errors in temperature. The variation in the melting point as a function of pressure is given by the Clausius–Clapyron equation

$$\left(\frac{dP}{dT}\right)_{\mathrm{coexist}}=\frac{\Delta H}{T\Delta V}. \tag{17}$$

Molecular dynamics simulations in the *NPT* ensemble were carried out for both the solid and the liquid phase at 1074 K and -30 MPa (the calculated coexistence pressure) from which ΔH and ΔV were determined. The enthalpy of fusion

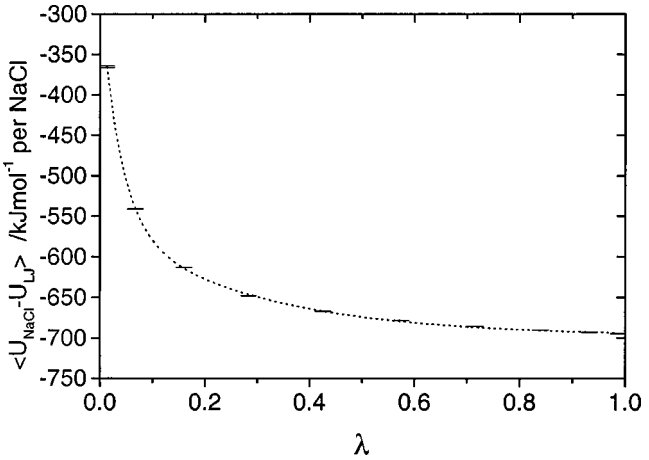

FIG. 5. Thermodynamic integration of LJ fluid ($\sigma=2.32$ Å and $\varepsilon=4.465$ kJ mol^{-1}) to NaCl liquid at 1074 K and 0.1 MPa pressure showing $\langle U_{\mathrm{NaCl}}-U_{\mathrm{LJ}}\rangle_\lambda$ as a function of the coupling parameter λ. The LJ fluid in reduced units corresponds to the state point $\rho^*=0.383$ and $T^*=2.0$. The sampling points in λ were defined by a 10-point Gauss–Legendre integration scheme that was used for the integration. The error bars represent the standard deviation in the ensemble average determined by block averaging.

$\Delta H=28.184$ kJ mol^{-1}/ion pair while the associated difference in volume $\Delta V=3811$ Å^3. Substitution of these values into the Clausius–Clapyron equation gives $dP/dT=3$ MPa/K which yields the melting point of 1064 ± 14 K at *ambient pressure*. The estimated relative error in the melting temperature is just over 1% and is similar in magnitude to the errors in the computed lattice energy and lattice parameters mentioned above.

It is well known that the rigid-ion potential as employed in this study does not fully reproduce the phonon dispersion curves of ionic solids. The implication is that this potential is not expected to accurately predict free energies for these systems and (consequently) their melting points. A fact that is less well appreciated is that the free energies of the solid phases of the alkali halides are dominated by the potential energy component, and the latter we know can be accurately predicted with a rigid-ion model using optimized parameters.

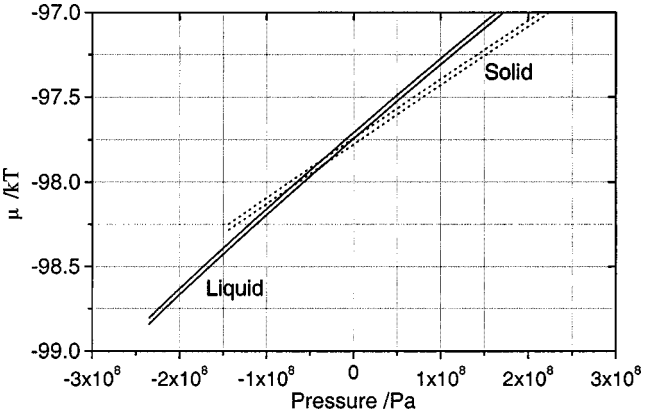

FIG. 6. Plot of the chemical potential μ displaying the associated uncertainty intervals corresponding to $\pm\sigma$ as a function of the pressure P for the liquid and the solid phase of NaCl at 1074 K. The melting transition occurs at the intersection where the chemical potentials and the pressures of the two phases are equal.

The shortcoming in the rigid-ion model is therefore responsible for errors in the entropy component of the free energy. The entropy component associated with the interaction potential, that is, other than the ideal (kinetic) part, is relatively small. Thus, the error associated with the rigid-ion model is in a quantity that makes only a small contribution to the overall free energy. Furthermore, as the same interaction potential is employed for both the solid and the liquid phase calculations, there is a possibility of cancellation of errors. The determined chemical potential of the NaCl solid phase is $-97.75k_\beta T$. Of this, the potential energy component is $-87.10k_\beta T$ while the ideal part is $-13.40k_\beta T$, leaving the entropy component arising from the interaction potential to be $2.75k_\beta T$. A 5% error in the latter quantity would have little or no effect on the melting point calculation. Hence, the ability of the Tosi–Fumi model to accurately reproduce the melting point of NaCl should not come as a surprise.

The calculation of the melting curve was expected to present some technical challenge. For the liquid phase, one cannot employ the expansion to ideal gas method, due to the strong, long-range interactions involved. Fortunately there is plenty of scope for developing alternative pathways for thermodynamic integration, which can be coupled with virtual particle insertion methods. The difficulty lies in deciding *a priori* which pathway is likely to yield the best accuracy and precision. Here, for the liquid phase, the thermodynamic integration of the LJ fluid to NaCl liquid proved to be significantly superior. This method probably also benefited by the judicious decision to select the LJ σ parameter for the LJ phase so as to make the first peak in the $g(r)$ of the LJ fluid to coincide with the Na–Cl ion pair correlation peak in the NaCl liquid, thus minimizing the disparity between the two states.

In summary, the melting point of NaCl has been calculated from the intersection of the chemical potential of the solid and the liquid phase. The study illustrates that the melting point of an ionic system can be calculated accurately by employing a judicious combination of free energy techniques, and represents an important first step towards investigating more complex, charged systems. The study also reveals that the Tosi–Fumi model for NaCl is excellent, enabling accurate reproduction of the experimental melting point.

ACKNOWLEDGMENTS

One of the authors (J.A.) is grateful to King's College London for a six-month sabbatical leave during which this work was initiated, and to the Netherlands Organization for Scientific Research (NWO) and the British Council for funding part of this work under the NWO-British Council Joint Scientific Research Program. The work of the FOM Institute is part of the research program of FOM and is made possible by financial support from NWO. The authors would like to thank Mauro Ferrario of University of Modena, Italy, for useful discussions.

[1] A. Z. Panagiotopoulos, N. Quirke, M. Stapleton, and D. J. Tildesley, Mol. Phys. **63**, 527 (1988).

[2] D. A. Kofke, Mol. Phys. **78**, 1331 (1993).
[3] D. A. Kofke, J. Chem. Phys. **98**, 4149 (1993).
[4] D. Frenkel, B. M. Mulder, and J. P. McTague, Phys. Rev. Lett. **52**, 287 (1984).
[5] R. Agrawal and D. A. Kofke, Mol. Phys. **85**, 43 (1995).
[6] P. G. Bolhuis and D. Frenkel, J. Chem. Phys. **106**, 666 (1997).
[7] M. G. Noro and D. Frenkel, J. Chem. Phys. **114**, 2477 (2001).
[8] E. J. Meijer, D. Frenkel, R. A. LeSar, and A. J. C. Ladd, J. Chem. Phys. **92**, 7570 (1990).
[9] B. Kuchta, K. Rohleder, D. Swanson, and R. D. Etters, J. Chem. Phys. **106**, 6771 (1997).
[10] B. Kuchta and R. D. Etters, Phys. Rev. B **47**, 14691 (1993).
[11] B. Kuchta and R. D. Etters, Phys. Rev. B **45**, 5072 (1992).
[12] L. A. Báez and P. Clancy, Mol. Phys. **86**, 385 (1995).
[13] M. J. Vlot, J. Huinink, and J. P. van der Eerden, J. Chem. Phys. **110**, 55 (1999).
[14] J. M. Polson and D. Frenkel, J. Chem. Phys. **111**, 1501 (1999).
[15] D. Alfe, M. J. Gillan, and G. D. Price, Nature (London) **401**, 462 (1999).
[16] D. Frenkel and A. J. C. Ladd, J. Chem. Phys. **81**, 3188 (1984).
[17] D. Frenkel and B. Smit, *Understanding Molecular Simulation: From Algorithms to Applications*, 2nd ed. (Academic, New York, 2002).
[18] J. M. Polson, E. Trizac, S. Pronk, and D. Frenkel, J. Chem. Phys. **112**, 5339 (2000).
[19] B. Widom, J. Chem. Phys. **39**, 2802 (1978).
[20] J. G. Kirkwood, J. Chem. Phys. **3**, 300 (1935).
[21] M. Ferrario, G. Ciccotti, E. Spohr, T. Cartailler, and P. Turq, J. Chem. Phys. **117**, 4947 (2002).
[22] K. S. Shing and K. E. Gubbins, Mol. Phys. **46**, 1109 (1982).
[23] F. G. Fumi and M. P. Tosi, J. Phys. Chem. Solids **25**, 31 (1964).
[24] M. P. Tosi and F. G. Fumi, J. Phys. Chem. Solids **25**, 45 (1964).
[25] J. Anwar, *ATOMH: An Object-Oriented Molecular Simulation Toolkit* (Computational Pharmaceutical Sciences Laboratory, King's College, London, 1995).
[26] H. Flyvbjerg and H. G. Petersen, J. Chem. Phys. **91**, 461 (1989).
[27] M. Parrinello and A. Rahman, J. Appl. Phys. **52**, 7182 (1981).
[28] L. Pauling, *The Nature of the Chemical Bond and the Structure of Molecules and Crystals: An Introduction to Modern Structural Chemistry* (Cornell University Press, Ithaca, NY, 1960), p. 526.
[29] CORIS-Projekt, Beitrag der Hoechst AG (Springer, Berlin).
[30] DETHERM Thermophysical Property Data Bank distributed by Dechema e.V., 2002.
[31] V. S. Urusov and V. V. Blinov, Izv. Akad. Nauk SSSR, Mekh. Zhidk. Gaza **12**, 278 (1970).
[32] L. W. Finger and H. King, Am. Mineral. **63**, 337 (1978).
[33] M. Yamada, M. Tago, S. Fukusako, and A. Horibe, Thermochim. Acta **218**, 401 (1993).
[34] Y. Zhang, Y. Han, and S. Wang, Thermochim. Acta **254**, 383 (1995).
[35] C. Qiyuan, Z. Wenming, C. Xinmin, G. Songqing, Y. Guanqun, Z. Huifang, and Y. T. Zhonglin, Thermochim. Acta **253**, 33 (1995).
[36] T. Grande, S. Aasland, and S. Julsrud, Thermochim. Acta **256**, 1 (1995).